pISSN 1598-298X
J Vet Clin 31(3) : 233-236 (2014)

Journal of Veterinary Clinics
www.ksvc.or.kr

Pulmonary Mineralization Secondary to Iatrogenic Hyperadrenocorticism in a Dog

Noh-won Park, Wook-hun Chung*, Jae-ik Han* and Ki-dong Eom[1]

College of Veterinary Medicine, Konkuk University, Seoul 143-701, Korea
**Nowon N Animal Medical Center, Seoul 139-816, Korea*

(Accepted: April 25, 2014)

Abstract : An 11-year-old, intact male Shih Tzu presented with obesity, thin hair coat, and abdominal distention. The patient had previously received corticosteroid therapy for dermatitis. Thoracic radiographs showed incidental findings of a generally diffuse bronchointerstitial pattern and markedly radiolucent pleural lines between the middle and caudal lung lobes, but clinical signs related to the thoracic radiographic findings were absent. Echogenicity of the hepatic parenchyma was increased and bilateral adrenal glands were not enlarged on ultrasonography. On computed tomography, the central regions of the lung lobes showed ground-glass attenuation, the peripheral regions of the lung lobes were relatively hypoattenuated compared with the central regions, and hyperattenuated nodules were distributed throughout the pulmonary parenchyma. Iatrogenic hyperadrenocorticism and secondary pulmonary mineralization was diagnosed on the basis of diagnostic imaging and adrenocorticotropic hormone stimulation test.

Key words **:** dog, hyperadrenocorticism, pulmonary mineralization.

Introduction

Hyperadrenocorticism may result in soft-tissue mineralization in dogs, with bronchial mineralization in 90% of canine patients and pulmonary mineralization in 40% (5). Pulmonary and bronchial mineralizations are commonly seen on thoracic radiographs and may be confused with geriatric changes (4,18,22). Survey thoracic radiography is a low-contrast technique and is less sensitive for confirmation of pulmonary mineralization than high-resolution computed tomography (HRCT), in which images are reconstructed with thin slice thickness and high definition, as well as nuclear scintigraphy (6,7,19). This report describes diagnostic imaging findings on computed tomography of generalized pulmonary mineralization secondary to iatrogenic hyperadrenocorticism.

Case

An 11-year-old, intact, male Shih Tzu weighing 6.5 kg was presented to Nowon N Animal Medical Center with anorexia and vomiting. The patient had received corticosteroid therapy for dermatitis at another hospital. Physical examination revealed obesity (body condition score, 4/5), thin hair coat, and abdominal distention as well as calcinosis cutis signs on dorsal cervical and thoracic skin regions. Thoracic auscultation was normal. Hemoglobin (18.2 g/dL; reference range, 12-18 g/dL) and platelets (710×10^9 /L; reference range, $175\text{-}500 \times 10^9$ /L) were increased on complete blood cell count. Serum chemistry showed increased ALKP (1,299 U/L; reference range, 23-212 U/L), ALT (452 U/L; reference range, 10-100 U/L), AST (117 U/L; reference range, 0-7 U/L), and GGT (110 U/L; reference range, 0-7 U/L).

Thoracic radiography revealed incidental findings of a generally diffuse bronchointerstitial pattern and markedly radiolucent pleural lines between the middle and caudal lung lobes (Fig 1). The margin of the liver was rounded on the lateral view of abdominal radiographs. Clinical signs related to thoracic radiographic findings were absent, so the patient was referred to the Veterinary Medical Teaching Hospital of Konkuk University for further diagnosis. On ultrasonography (Prosound alpha7, Aloka Co. Ltd., Tokyo, Japan), echogenicity of the hepatic parenchyma was similar to that of the spleen (Fig 2A and B). Renal cortices were hyperechoic bilaterally, but blood flow distribution of the cortices appeared normal on color Doppler mode ultrasonography (Fig 2C and D). There was no adrenal gland enlargement (caudal pole diameter, 4.7 mm). CT (LightSpeed Plus, GE Medical Systems LLC, Waukesha, WI, USA) was performed for further evaluation of the lung lesions. A high spatial reconstruction protocol was used to enhance detail of the pulmonary parenchymal structure. The central regions of the lung lobes showed ground-glass attenuation, and the peripheral regions of the lung lobes were relatively hypoattenuated compared with the central regions; hyperattenuated miliary nodules were distributed throughout the pulmonary paren-

[1]Corresponding author.
E-mail : eomkd@konkuk.ac.kr

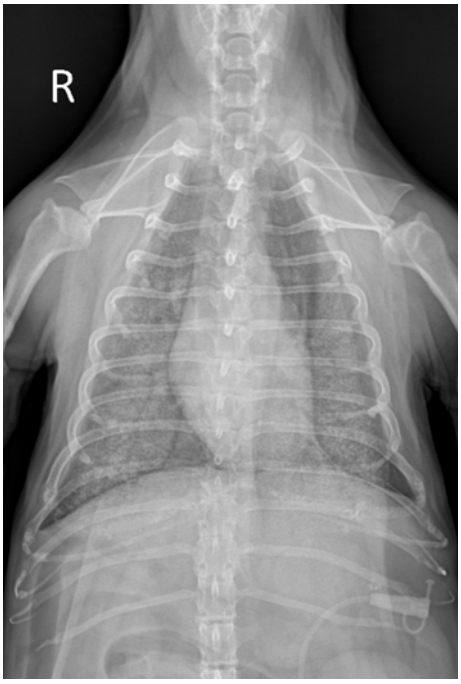

Fig 1. Ventrodorsal thoracic radiograph of the patient in the humanoid position. A generally diffuse bronchointerstitial pattern is present in the entire lung.

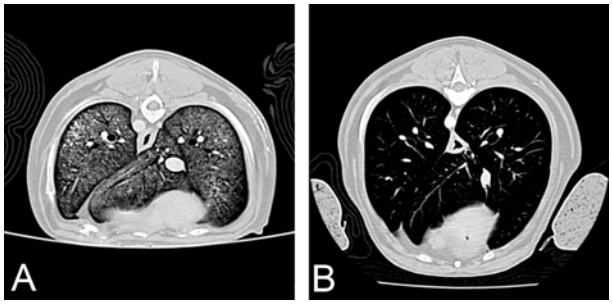

Fig 3. Transverse computed tomographic image at the level of the cranial aspect of the diaphragm of the patient in this case (A) and another patient considered normal regarding pulmonary findings with the same window width and window level (B). The pulmonary parenchyma of the hyperadrenocorticism case shows diffuse ground-glass attenuation in bilateral caudal and accessory lung lobes and hyperattenuated miliary nodules in the dorsal region of the left caudal lung lobe.

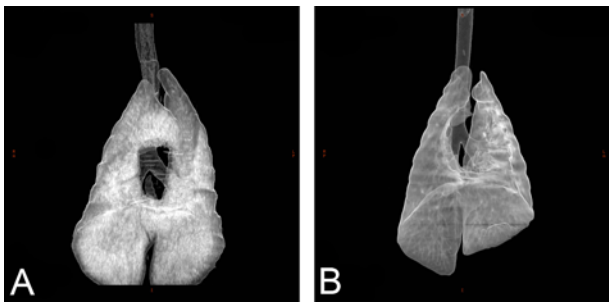

Fig 4. Three-dimensional reconstructed image of the lung of the patient in this case (A) and another patient considered normal regarding pulmonary findings with the same window width and window level (B). The entire lung lobes are mineralized in the hyperadrenocorticism case compared with the normal patient.

chyma (Fig 3). The bronchioles and blood vessels were well delineated from the pulmonary parenchyma. Diffuse attenuation value increase was revealed in entire lobes of the lung on pulmonary 3-dimensional reconstruction images (Fig 4). Mean Housefield Unit value of the pulmonary parenchyma in the patient was −495.62 ± 330 HU (range, −1007-86 HU). That was higher than that in another patient of that lung was considered as normal (−811.73 ± 88.16 HU; range, −934 - −622 HU).

An adrenocorticotropic hormone stimulation test (SNAP cortisol test kit, IDEXX laboratories Inc., Westbrook, Maine, USA) was performed after CT examination by administering tetracosactrin (250 μg IM; Synacthen, Dalim Bio Tech, Co., Ltd., Seoul, Korea). Cortisol levels before and 1 hour after adrenocorticotropic hormone stimulation were 0.5 and 2.5 uL/dL, respectively (reference range, 0.5-10 uL/dL). The patient was diagnosed with iatrogenic hyperadrenocorticism with secondary pulmonary mineralization and was treated with trilostane (2.5 mg/kg PO; Vetoryl® 60 mg, Dales Pharmaceuticals, Ltd., Skipton, UK) for 3 months. Follow-up examination was performed 3 months after the initial adrenocorticotropic stimulation test. According to the client, the

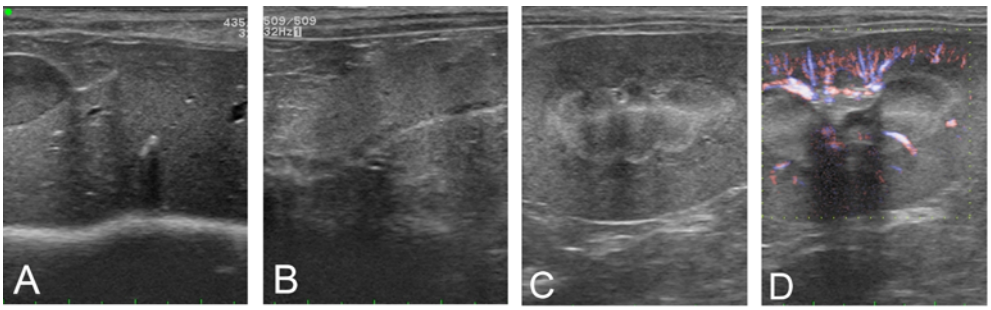

Fig 2. Ultrasonographic images of liver (A), spleen (B), and left kidney (C and D). The hepatic parenchyma is hyperechoic, with similar echogenicity to that of the splenic parenchyma. The left renal cortex is hyperechoic, but there is a normal vascular reaction on color Doppler ultrasonography.

chief complaints of vomiting and anorexia were resolved after treatment administration. Cortisol levels were within the reference range on the adrenocorticotropic hormone stimulation test (pre- and 1-hour-post-adrenocorticotropic hormone stimulation, 2.3 uL/dL and 8.7 uL/dL, respectively; reference range, 0.5-10 uL/dL), but thoracic radiographic examination findings were identical to those 3 months previously despite improved clinical signs and cortisol levels.

Discussion

Pulmonary mineralization is categorized into 4 types according to pathogenic mechanism: dystrophic, metastatic, idiopathic, and iatrogenic (2). The pulmonary mineralization presented in this case was considered dystrophic mineralization because of the presence of hepatopathy and increased renal cortical echogenicity as well as the ACTH stimulation test result. Dystrophic mineralization is caused by abnormal calcium and phosphorus deposition in catabolic protein matrix due to excessive cortisol in hyperadrenocorticism (5). Dystrophic mineralization is associated with calcinosis cutis and mineralization of tracheal rings, bronchial walls, mucosa, kidney, and liver (1,13). The presented case showed calcinosis cutis and mineralization of tracheal rings, bronchial walls, pulmonary parenchyma, and kidneys. Radiographic findings of dystrophic pulmonary mineralization secondary to hyperadrenocorticism include interstitial pulmonary parenchymal pattern and ectopic calcification of bronchial walls and tracheal rings. However, these findings are not usually as pronounced as in this case and are often confused with normal geriatric changes (14). Furthermore, survey thoracic radiography has low sensitivity for the diagnosis of pulmonary mineralization because of low contrast exposure techniques (19).

Nuclear scintigraphy using 99mTechnitium-methylene disphosphonate (99mTc-MDP) and HRCT is used to diagnose pulmonary mineralization in human medicine (19). Nuclear scintigraphy using 99mTc-MDP exposes mineralized lesions by binding to hydroxyapatite crystals in the extracellular space of soft tissue (3,20), and 99mTc-MDP uptake can clearly show mineralized lesions in the lung. Nuclear scintigraphy was not available in this case, and HRCT was performed instead. HRCT involves image acquisition with a thin slice thickness of 1-2 mm and high spatial frequency reconstruction algorithm (8,17). The image acquisition protocol in the presented case included a 1.25 mm slice thickness coupled with a high spatial reconstruction algorithm. HRCT is more sensitive for diagnosis of pulmonary parenchymal and airway disease than is conventional pulmonary CT (15). On HRCT, pulmonary mineralization appears as multiple calcified and/or noncalcified nodules, ground-glass opacification areas, and relatively dense areas of consolidation (6). The findings of CT images of the present case were similar to those of previous study. Although not present in this case, respiratory distress in hyperadrenocorticism due to various pathogenic mechanisms has been reported previously.

Pulmonary diffusion impairment due to pulmonary mineralization and thromboembolism secondary to hyperadrenocorticism induces ventilation-perfusion mismatch, which results in hypoxia (1). Hyperadrenocorticism also causes respiratory distress because of increased pressure on the diaphragm due to hepatomegaly, respiratory muscle weakness, and decreased respiratory excursion due to fat deposition on the thoracic wall (5). Thrombocytosis was present in the complete blood cell count of this case, and hyperadrenocorticism is associated with development of pulmonary thromboembolism (4,16). Clinical signs associated with pulmonary thromboembolism include dyspnea, tachypnea, and depression together with thrombocytosis on CBC and increased hypoxemia and hypocapnia on arterial blood-gas analysis (11). Findings on thoracic radiography are inconsistent in pulmonary thromboembolism, but pulmonary infiltrate, oligemia, and decreased vascular pattern have been frequently reported (10,21). CT angiography is a highly sensitive diagnostic tool for pulmonary thromboembolism, which is recognized by round contrast medium filling defects in the pulmonary vasculature (9,12). This case displayed thrombocytosis without pulmonary thromboembolism because filling defects were not evident on CT angiography. However, thrombocytosis is considered associated with the hyperadrenocorticism in the presented case, and the patient is at risk of respiratory distress due to pulmonary thromboembolism in the future.

Conclusion

This report describes the diagnosis of pulmonary mineralization secondary to iatrogenic hyperadrenocorticism. Pulmonary mineralization is characterized by a diffuse bronchointerstitial pattern on thoracic radiography and ground glass attenuation in the pulmonary parenchyma with hyperattenuated nodules on CT. Pulmonary thromboembolism secondary to hyperadrenocorticism is associated with a high incidence of respiratory distress with poor prognosis, so close follow-up is needed regarding respiratory distress.

Acknowledgements

This study was supported by Veterinary Science Research Institute of the Konkuk University.

References

1. Berry CR, Ackerman N, Monce K. Pulmonary mineralization in four dogs with Cushing's syndrome. Vet Radiol Ultrasound 1994; 35: 10-16.
2. Bogart SD. Disseminated pulmonary calcinosis with pulmonary alveolar microlithiasis. N Y state J Med 1980; 80: 1283-1284.
3. Brown ML, Swee RG, Olson RJ, Bender CE. Pulmonary uptake of 99mTc diphosphonate in alveolar microlithiasis. Am J Roentgenol 1978; 131: 703-704.
4. Burns MG, Kelly AB, Hornof WJ, Howerth EW. Pulmonary

artery thrombosis in three dogs with hyperadrenocorticism. J Am Vet Med Assoc 1981; 178: 388-393.
5. Capen CC. The endocrine glands. In: Pathology of domestic animals, 3rd Ed. Orlando: Academic Press. 1985: 287-304.
6. Chan ED, Morales DV, Welsh CH, McDermott MT, Schwarz MI. Calcium deposition with or without bone formation in the lung. Am J Respir Crit Care Med 2002; 165: 1654-1669.
7. Chung MJ, Lee KS, Franquet T, Muller NL, Han J, Kwon OJ. Metabolic lung disease: Imaging and histopathologic findings. Eur J Radiol 2005; 54: 233-245.
8. Corcoran HL, Renner WR, Milstein MJ. Review of high resolution of the lung. Radiographics 1992; 12: 917-939.
9. Davidson BL, Rozanski EA, Tidwell AS, Hoffman AM. Pulmonary Thromboembolism in a Heartworm-Positive Cat. J Vet Intern Med 2006; 20: 1037-1041.
10. Flückiger MA, Gomez JA. Radiographic findings in dogs with spontaneous pulmonary thrombosis or embolism. Vet Radiol Ultrasound 1984; 25: 124-131.
11. Goggs R, Benigni L, Fuentes VL, Chan DL. Pulmonary thromboembolism. J Vet Emerg Crit Care 2009; 19: 30-52.
12. Goodman LR, Curtin JJ, Mewissen MW, Foley WD, Lipchik RJ, Crain MR, Sagar KB, Collier BD. Detection of pulmonary embolism in patients with unresolved clinical and scintigraphic diagnosis: helical CT versus angiography. Am J Roentgenol 1995; 164: 1369-1374.
13. Huang HP, Yang HL, Liang SL, Lien YH, Chen KY. Iatrogenic hyperadrenocorticism in 28 dogs. J Am Anim Hosp Assoc 1999; 35: 200-207.
14. Huntley K, Frazer J, Gibbs C, Gaskell CJ. The radiographic features of canine Cushing's syndrome: A review of forty-eight cases. J Small Anim Pract 1982; 23: 369-380.
15. Kazerooni EA. High-resolution CT of the lungs. Am J Roentgenol 2001; 177: 501-519.
16. King RR, Mauderly JL, Hahn FF, Wolff RK, Muggenburg BA, Pickrell JA. Pulmonary function studies in a dog with pulmonary thromboembolism associated with Cushing's disease. J Am Anim Assoc 1985; 21: 555-562.
17. Mayo JR. High resolution computed tomography. Technical aspects. Radiol Clin North Am 1991; 29: 617-621.
18. Penninck DG, Feldman EC, Nyland TG. Radiographic features of canine hyperadrenocorticism caused by autonomously functioning adrenocortical tumors: 23 cases (1978-1986). J Am Vet Med Assoc 1988; 192: 1604- 1608.
19. Schwarz LA, Tidwell AS. Alternative imaging of the lung. Clin Tech Small Anim Pract 1999; 14: 187-206.
20. Turktas H, Ozturk C, Guven M, Ugur P, Erzen C. Pulmonary alveolar microlithiasis with the absence of technetium-99m MDP of lungs. Clin Nucl Med 1988; 12: 883-885.
21. Westermark N. On the roentgen diagnosis of lung embolism. Acta Radiol 1938; 19: 357-372.
22. Widmer WR, Guptil L. Imaging techniques for facilitating diagnosis of hyperadrenocorticism in dogs and cats. J Am Vet Med Assoc 1995; 206: 1857-1864.

개에서 발생한 의인성 부신피질기능항진증과 속발성 폐 석회화 진단 1례

박노운 · 정욱헌* · 한재익* · 엄기동[1]

건국대학교 수의과대학, *노원 N 동물의료센터

요 약 : 피부염 치료를 위해 스테로이드를 처방받은 경력이 있는 11년령 수컷 시추가 비만, 얇은 피모, 복부 팽만으로 내원하였다. 방사선 사진상 폐야 전반에 기관지-간질패턴과 뚜렷한 흉막음영이 관찰되었으나 신체검사상 이와 관련한 증상은 보이지 않았다. 복부 초음파상 부신은 정상크기이며 간실질의 에코성 상승을 나타내었다. 컴퓨터 단층촬영상 폐 중앙부는 간유리음영을 나타내었으며 변연부는 중앙부에 비해 저감약성을 띄고, 고감약성 결절음영이 폐 실질 전반에 산재되어 있었다. 영상진단학적 소견과 부신피질자극 호르몬 검사결과를 바탕으로 의인성 부신피질기능항진증과 속발성 폐 석회화로 진단하였다.

주요어 : 개, 부신피질기능항진증, 폐 석회화